http://mmg.tversu.ru ISSN 2311-1275

Mathematical Modelling and Geometry

Volume 2, No 3, p. 1 – 10 (2014)

Mathematical Modeling of Track Formation in Superconductor in Cylindrical Coordinates

J. Pribiš[1,2]

[1] Technical university of Košice, Košice, Slovakia
[2] Joint Institute for Nuclear Research, Dubna, Russia

e-mail: jan.pribis@tuke.sk

Received 1 September 2014, in final form 11 September. Published 12 September 2014.

Abstract. Further development of the thermal explosion model (TEM) describing track formation processes in high-T_c superconductors is suggested. Information on the temperature dependence of electron thermal diffusivity in $YBa_2Cu_3O_{7-x}$ is obtained by solving an inverse problem of reproducing measured track radii within the framework of TEM. An influence of the velocity of the incident ion on the damage production in $YBa_2Cu_3O_{7-x}$ is discussed. For numerical calculations a finite difference method was used.

Keywords: Heat transfer, track formation, finite difference method.

PACS numbers: 02.60.Cb, 02.60.Lj, 02.70.Bf

1. Introduction

Nanodimensions ion track technologies are now of great importance for their enabling increase the critical current density in high-T_c superconductors. In spite of the manifest practical significance, no satisfactory theory of track formation for these materials exists so far. Although different mechanisms were suggested till now, thermal spike model (TSM) was demonstrated to be one of the most matchable for this purpose (see [1, 2, 3] and references therein). Mathematical modeling of track formation in $YBa_2Cu_3O_{7-x}$ using TSM revealed some unexpected features of the process such as impossibility to formulate an appropriate Stephan problem, existence of the electronic quenching phenomenon which results in supersensitivity of track radii to small variations of electron diffusivity value [2], and others. It was shown in [3] that taking into account superheating nonequilibrium processes allows one to stabilize the model and obtain a quantitative description of tracks in $YBa_2Cu_3O_{7-x}$ with both elliptical and circular cross sections.

In present paper, another even more crucial problem of theory is considered. The fact is that electron thermal diffusivity, D_e, was considered previously as an adjustable parameter of thermal spike and thermal explosion models for varying types and energies of impinging ions. Meanwhile, the self-consistency of the theory requires to use a single function, depending on electron temperature in the superconductor, $D_e(T_e)$, for the whole bulk of data. We show here that such a function exists and takes quite reasonable physical values.

Since a comprehensive description of the theory can be found elsewhere [1, 2, 3], here we give only a brief outline of its main features.

2. Thermal Spike and Thermal Explosion Models

In the thermal spike model (TSM), the following system of two coupled nonlinear differential equations for electron, T_e, and atom, T_i, temperatures is assumed:

$$\rho C_e(T_e)\frac{\partial T_e}{\partial t} = \frac{1}{r}\frac{\partial}{\partial r}\left[rK_e(T_e)\frac{\partial T_e}{\partial r}\right] + \frac{1}{r^2}\frac{\partial}{\partial \varphi}\left[K_e(T_e)\frac{\partial T_e}{\partial \varphi}\right] - g\cdot(T_e - T_i) + q(r,\varphi,t), \tag{1}$$

$$\rho C_i(T_i)\frac{\partial T_i}{\partial t} = \frac{1}{r}\frac{\partial}{\partial r}\left[rK_i(T_i)\frac{\partial T_i}{\partial r}\right] + \frac{1}{r^2}\frac{\partial}{\partial \varphi}\left[K_i(T_i)\frac{\partial T_i}{\partial \varphi}\right] + g\cdot(T_e - T_i). \tag{2}$$

Parameters of the model were extracted from different independent experiments employing existing theory [2]. Initial conditions are chosen in a form

$$T_e(r,0) = T_i(r,0) = T_0,$$

and boundary conditions are

$$(\partial T_e/\partial r)_{r=r_{min}} = (\partial T_i/\partial r)_{r=r_{min}} = 0,$$

$$T_e(r_{max}, t) = T_i(r_{max}, t) = T_0,$$

where T_0 is temperature of the environment and no-heat-transfer condition at the center of track $r = r_{min}$ is taken into account. Parameter $r_{min} = 0.1$ nm is introduced to avoid difficulties with description of energy deposition at point $r = 0$, and $r_{max} = 10^{-5}$ cm is a physical infinity as used here.

When the direction of an incident ion is parallel to c axis, one can ignore the φ-dependence, and the system (1)–(2) is reduced to that used in [2] for description of tracks with circular cross sections. When the incident ion is parallel to [100] or [010] directions, the defects appear elliptical in shape [4]. This fact was explained by an anisotropy of the thermal conductivity of $YBa_2Cu_3O_{7-x}$ in the a-c and b-c planes [3]. Corresponding calculations were fulfilled in the frame of thermal explosion model (TEM) which turns out to be more stable than TSM against small variations of electron thermal diffusivity parameter, D_e.

3. Description of energy deposition

In view of an experiment [5], where the projectile velocity influence on track formation was reported, we developed a model of energy source, $q(r, \varphi, t)$, included in right side of equation (1), more exact than those usually used in calculations of this type. Namely, the space-time distribution of energy deposition upon electrons, accounting for its dependence on the projectile velocity, was simulated. The corresponding code (in FORTRAN) and its description is available [8]. A quality of simulation can be estimated regarding the following parameters:

1. for all of considered ions, stopping power calculated as radially integrated dose distribution is in agreement with SRIM code [9] within 25 % accuracy (the precision of SRIM code itself is believed to be about 15 %);

2. radial distribution of dose around the path of a heavy ion matches the delta-ray model [6] of track structure, which is widespread in radiation dosimetry, within 10 % precision;

3. the model incorporates energy deposition due to primary excitations and ionization of atoms, and δ-electron kinetic energy transfer. According to it, the primary excitations contribute essentially, about 50 %, in the region r $<$ 10 nm. For r $>$ 10 nm investment of δ-electrons entirely dominates;

4. the δ-electron dynamics, suggested in [7], was used to find a time dependence of energy deposition at a given point, r, around the center of track. Thus, a time of energy release was slightly delayed for about 50 % of energy deposition corresponding to the primary excitations. One can ignore this inaccuracy since it is compensated (and even overcompensated) by the time necessary for decays of primary excitations via the Auger transitions.

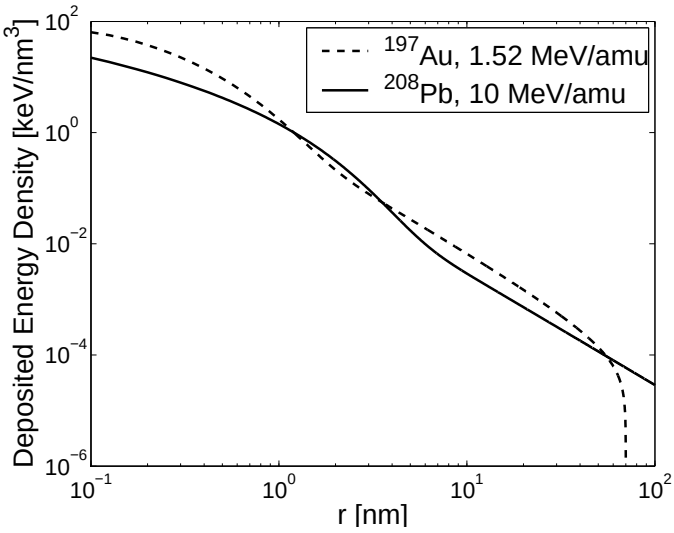

Figure 1: Dependence of energy deposition on distance, r, from the center of track in $YBa_2Cu_3O_{7-x}$ for two different bombarding ions having nearly the same energy deposition per unit of ion's path, $\mathrm{d}E/\mathrm{d}x = 43.7$ and 44.1 keV/nm for Pb and Au, accordingly.

An example of calculations in the frame of this model is shown in Fig. 1, where two different ions with approximately equal stopping power, $\mathrm{d}E/\mathrm{d}x$ is considered. The velocity effect is seen as lower and wider distribution of energy deposition (in the range not very far from the track center) for a faster ion, as it was described in [5]. One can readily understand the phenomenon, as far as the faster ion is able to impose electrons more initial velocity and, therefore, push them further away from the center of track. Corresponding electron temperatures, $T_e(r = 0, t)$, obtained as a solution of system (1)–(2) with these energy depositions are shown in Fig. 2. One can see that energy deposition in the interval $r < 1$ nm is the most influencing on electron temperature in the center of track and, as numerical experiments also revealed, on a value of the track radius.

4. Properties of electron subsystem

The basic equations (1)–(2) are energy conservation laws which admit both quantum and classical physics specification implemented in thermal physics constants. Thermal capacity of electrons is taken here in the form,

$$\rho C_e = \gamma T_e \tag{3}$$

with an experimentally estimated value of Sommerfeld's parameter, $\gamma = 2.4 \pm 0.8 \cdot 10^{-4}$ J/(cm^3 K^2) [10]. According to [11], the electronic thermal conductivity of $YBa_2Cu_3O_{7-x}$ equals to $K_e = 2.5 \cdot 10^{-2}$ W/(cm K) in plane (001) at $T_e \simeq 300$ K. This, with taking into account the previous estimation for γ, corresponds to

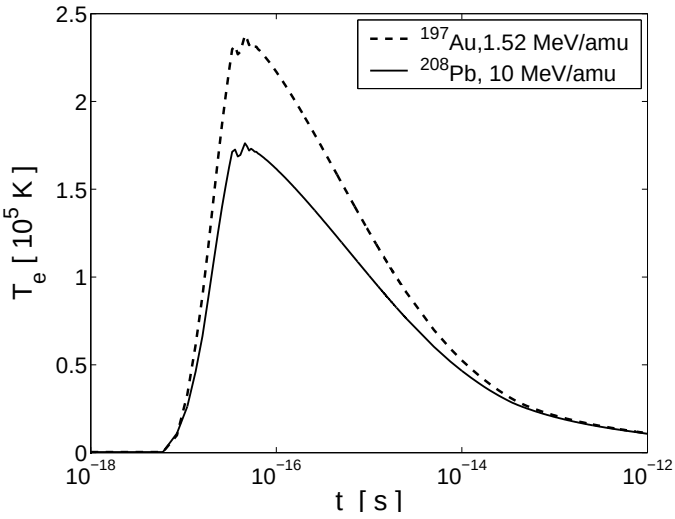

Figure 2: Electron temperatures as functions of time at the center of track in $YBa_2Cu_3O_{7-x}$ for the same bombarding ions as in Fig. 1 found in the frame of TEM.

the value of electron diffusivity $D_e \equiv K_e/\rho C_e = 0.26 \div 0.52$ cm^2/s. At higher temperatures K_e and D_e are unknown yet. The choice $D_e = 1$ – 2 cm^2/s accepted in Caen version of TSM was motivated by reasons that hot electrons penetrate into the conduction band where they behave like in metals [12], and values of this order are often suggested for other substances at high temperatures, including metals themselves [13].

Thermal diffusivity in $YBa_2Cu_3O_{7-x}$ as function of electron temperature, found via minimization of deviation of the theoretical track radii from experimental ones, is shown in Fig. 3. It satisfies the requirement to be $\simeq 1$ cm^2/s at high temperatures, as it was predicted in [12, 13], and demonstrates a monotonous growth at $T_e > 10^4$ K, in qualitative agreement with [14]. A decrease of function $D_e(T_e)$ from $D_e \simeq 0.26 \div 0.52$ at $T_e = 300$ K to $D_e \simeq 0.01$ K at $T_e = 10^4$ K is slightly unexpected, though quite possible, and is a non trivial prediction of this variant of TEM.

In Fig. 4 we can sea that electron temperature for the indicated ion (and for all others specified below) is lower than 10^4 K at the moment $t = t_b$. According to Fig. 3, this means that the value of D_e is very small in the final stage of track boundary formation, and it is another reason for turning off the electron quenching.

The variable τ describing the rate of energy transfer from electron to atoms can be retrieved from existing experimental data as follows. Due to linear dependence of ρC_e on T_e, function $\tau(T_e)$ acquires the same linear form, $\tau = (\gamma/g)\, T_e \equiv \alpha T_e$, as it was predicted by Allen's theory [15], where

$$\tau = \frac{\pi}{3}\frac{k_B\,\hbar}{\lambda' < \omega^2 >} T_e.$$

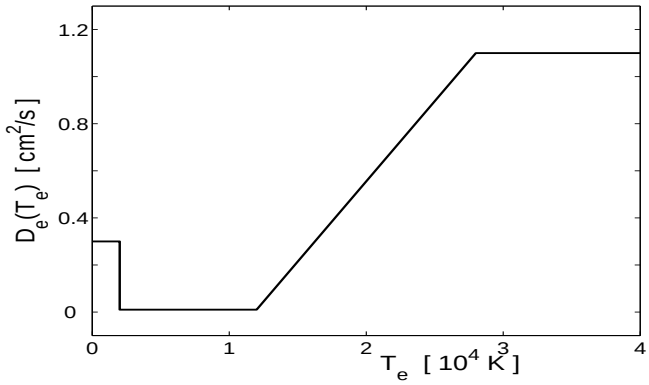

Figure 3: Thermal diffusivity in $YBa_2Cu_3O_{7-x}$ as function of electron temperature, T_e, found from the requirement imposed on TEM to account for experimental track radii.

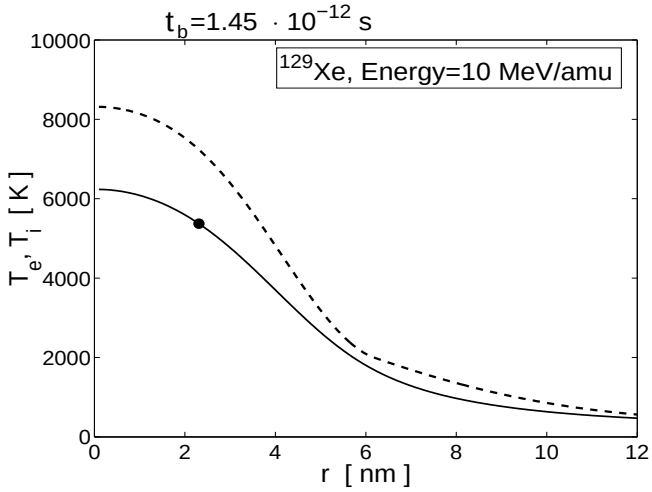

Figure 4: $T_e(r)$ (dashed curve) and $T_i(r)$ (solid curve) distributions for ion ^{129}Xe at 10 MeV/amu in $YBa_2Cu_3O_{7-x}$. Theoretical radius of track is shown as a point on solid curve at the temperature of superheating $T_{sh} \simeq 5370$ K.

Using the experimental value of $\lambda' < \omega^2 >= 475 \pm 30$ meV^2 established in [16], one can estimate parameter α from Allen's theory,

$$\alpha = (1.28 \pm 0.06) \cdot 10^{-16} \text{s/K}.$$

Then electron-atom coupling constant, g, containing in the basic equations (1) and (2) is

$$g = \frac{\gamma}{\alpha} = (1.9 \pm 0.7)\ 10^{12} \frac{\text{J}}{\text{s cm}^3\ \text{K}}.$$

Values of $\tau(T_e)$ at the moving boundary of the molten region for Pb at 10 MeV/amu is shown depending on time in Fig. 5.

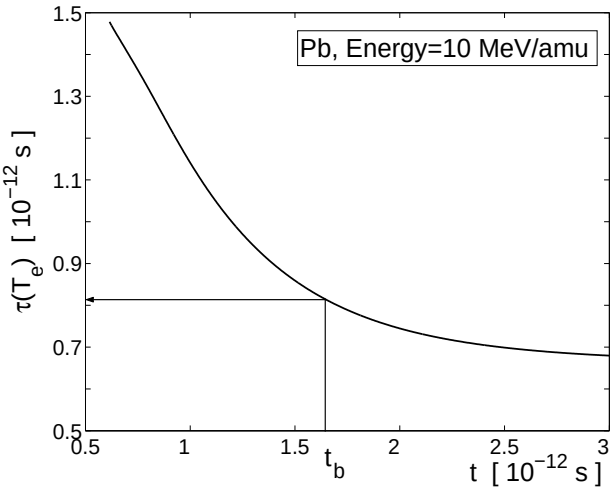

Figure 5: Electron-atom relaxation time, τ, at the moving boundary of the molten region for ion ^{208}Pb at 10 MeV/amu in $YBa_2Cu_3O_{7-x}$. At the moment $t = t_b$ when the molten region size reaches its maximum, the value of $\tau(t)$ is less than t_b itself.

5. Description of atomic subsystem and track radii

Properties of the atomic subsystem are described in more details in [2]. Here we give only a brief overview of them. For lattice thermal capacity, the Dulong-Petit value, $\rho C_i = 3.1$ J cm^{-3} K^{-1}, was taken, where $\rho = 6.39$ g cm^{-3} is density of the material. Thermal conductivity of the atomic system, K_i, was chosen in accordance with [11, 15], $K_i = 5.6\times10^{-2}$ J(s cm K)$^{-1}$. To take into account the melting process in TSM, we define the effective specific heat (see sect. 3)

$$C_i^{eff} = C_i + L\delta(T^* - T_i),$$

where $L = (810 \pm 5)$ kJ/mol ≈ 1.22 kJ/g is a change of enthalpy accompanying melting of $YBa_2Cu_3O_{7-x}$ [17], and $T^* = 1070$ C is the temperature at which melting begins, found by the real time neutron diffraction analysis [18]. The equation (2) can now be rewritten in the form

$$\left(1 + \frac{L}{C_i}\delta(T^* - T_i)\right)\frac{\partial T_i}{\partial t} = D_i\frac{\partial^2 T_i}{\partial r^2} + \frac{D_i}{r}\frac{\partial T_i}{\partial r} + \frac{T_e - T_i}{\tau_i}, \qquad (4)$$

where $D_i \approx 1.8\ 10^{-2}$ cm^2/s is thermal diffusivity of the atomic subsystem, $\tau_i = \rho C_i/g \approx 1.6\ 10^{-12}$ s is a characteristic electron-atom excitation time. For numerical solution of (4), a regularization of δ-function was done by the instrumentality of Gauss distribution with $\sigma = 5$ K, and melting was considered to take place in the interval $T_i = T^* \pm 4.5\sigma$. In the TEM framework, δ-function in l.h.s. of (4) is omitted, but melting is considered to be at $T_{sh} = 4T^*$.

Experimentally observed radii of tracks, r_{exp}, in $YBa_2Cu_3O_{7-x}$ single crystal with [001] axis oriented parallel to the incident ion beam are also given in the

Ion	Energy MeV/amu	$\mathrm{d}E/\mathrm{d}x$, SRIM keV/nm	$\mathrm{d}E/\mathrm{d}x$, THEOR keV/nm	r_{exp} nm	r_{th} nm
^{129}Xe	1.3	26.2	30.5	2-3	3.19
^{129}Xe	2.6	30	31.2	2.5	2.95
^{129}Xe	10	27.9	25.7	1.3	2.31
^{129}Xe	27	18.7	17.7	1.3	1.37
^{129}Xe	41	14.8	14.3	0.56	0.30
^{208}Pb	3.7	43.7	47.8	4	4.30
^{208}Pb	10	42.5	43.7	3	3.91
^{208}Pb	20	37	37	3.5	3.56
^{208}Pb	25	34.5	34.4	3	3.43
^{197}Au	1.52	36.2	44.1	3	4.42

Table 1: Experimentally observed radii of tracks, r_{exp}, in $YBa_2Cu_3O_{7-x}$ single crystal taken from [19] and results of their theoretical description, r_{th}. Energy deposition $\mathrm{d}E/\mathrm{d}x$, calculated using our code [8], is compared with results of SRIM-2013 [9]. Thermal diffusivity of electrons, $D_e \equiv K_e/\rho C_e$, was adjusted to reproduce r_{exp}, see Fig. 3.

numerical form in Table 1. Comparing pairs of rows in the Table for ^{129}Xe at energies 2.6 and 10, 1.3 and 10, 27 and 41 MeV/amu, which have nearly the same values of $\mathrm{d}E/\mathrm{d}x$, one can see that differences of track radii, both experimental and theoretical ones, for each pair of energies are relatively bigger than corresponding differences of $\mathrm{d}E/\mathrm{d}x$, and this is also true for ions of ^{208}Pb at 3.7 and 10 MeV/amu. Our observations agree with the conclusion of [5], drawn for the ion damages in $Y_3Fe_5O_{12}$, that "such a deviation might be explained by the effect of the energy deposition being more localized for the low-velocity ions than for the high velocity ions".

6. Conclusion

Numerical calculations are carried out on grid of variables r, φ and t with constant with spatial, angle and time steps h_r, h_φ and h_t, respectively:

$$r_j = r_{\min} + j \cdot h_r, \quad j = 0, \ldots, n_r, \quad h_r = (r_{\max} - r_{\min})/n_r,$$

$$\varphi_k = k \cdot h_\varphi, \quad k = 0, \ldots, n_\varphi, \quad h_\varphi = \pi/2/n_\varphi,$$

$$t_l = l \cdot h_t, \quad l = 0, \ldots, n_t, \quad h_t = t_{\max}/n_t,$$

where $r \in [r_{\min}, r_{\max}]$, $\varphi \in [0, \pi/2]$, $t \in [0, t_{\max}]$ n_r, n_φ and n_t are numbers of partitions.

For numerical solution, the system (3), (4) was approximated by the following explicit finite-difference scheme [20]:

$$\rho C^l_{e_{j,k}} \frac{T^{l+1}_{e_{j,k}} - T^l_{e_{j,k}}}{h_t} = \frac{1}{r_j}\Lambda_1 \left[r_j K^l_{e_{j,k}} T^l_{e_{j,k}} \right] + \frac{1}{r_j^2}\Lambda_2 \left[K^l_{e_{j,k}} T^l_{e_{j,k}} \right] - g^l_{j,k}(T^l_{e_{j,k}} - T^l_{i_{j,k}}) + q^l_{j,k}, \tag{5}$$

$$\rho C^l_{i_{j,k}} \frac{T^{l+1}_{i_{j,k}} - T^l_{i_{j,k}}}{h_t} = \frac{1}{r_j}\Lambda_1 \left[r_j K^l_{i_{j,k}} T^l_{i_{j,k}} \right] + \frac{1}{r_j^2}\Lambda_2 \left[K^l_{i_{j,k}} T^l_{i_{j,k}} \right] + g^l_{j,k}(T^l_{e_{j,k}} - T^l_{i_{j,k}}), \tag{6}$$

where

$$\Lambda_1(r_j K^l_{j,k} T^l_{j,k}) = \frac{1}{h_r}\left[r_{j+\frac{1}{2}} K^l_{j+\frac{1}{2},k} \frac{T^l_{j+1,k} - T^l_{j,k}}{h_r} - r_{j-\frac{1}{2}} K^l_{j-\frac{1}{2},k} \frac{T^l_{j,k} - T^l_{j-1,k}}{h_r} \right],$$

$$\Lambda_2(K^l_{j,k} T^l_{j,k}) = \frac{1}{h_\varphi}\left[K^l_{j,k+\frac{1}{2}} \frac{T^l_{j,k+1} - T^l_{j,k}}{h_\varphi} - K^l_{j,k-\frac{1}{2}} \frac{T^l_{j,k} - T^l_{j,k-1}}{h_\varphi} \right],$$

$$T^l_{j,k} = T(r_j, \varphi_k, t_l),\ C^l_{j,k} = C(T^l_{j,k}),\ K^l_{j,k} = K(T^l_{j,k}),\ g^l_{j,k} = g(T^l_{j,k}),\ q^l_{j,k} = q(r_j, \varphi_k, t_l)$$

$$r_{j\pm\frac{1}{2}} = \frac{r_j + r_{j\pm1}}{2},\ K^l_{j\pm\frac{1}{2},k} = \frac{K(T^l_{j,k}) + K(T^l_{j\pm1,k})}{2},\ K^l_{j,k\pm\frac{1}{2}} = \frac{K(T^l_{j,k}) + K(T^l_{j,k\pm1})}{2}$$

At present further improvement of TEM for track formation in $YBa_2Cu_3O_{7-x}$ runs into experimental ambiguities which could be removed by new measurements with a single sample and a uniform method of measuring, for different impinging ions. Inaccuracy of calculations of energy deposition, dE/dx, is another possible field of activity. Theoretical ambiguities are even more impressive, than in Table 1, if one considers energy release at $r \leq 1$ nm, which is the most-influencing-on-track-formation domain.

In conclusion, the high sensitivity of theoretical track radii to small changes of D_e found firstly in [2] is not a defect of TSM and TEM, as it may appear, but a real physical effect conditioned by near threshold formation of tracks in $YBa_2Cu_3O_{7-x}$. Under these circumstances, a small increase of D_e leads to artificial overcooling of the material and, as a result, to reduction, or even total collapse, of the melting region. Another false overcooling proved to be, however, in the previous variant of TSM and TEM [2, 3] due to ignoring $D_e(T_e)$ dependence. This ignoring exhibits in assigning to D_e at relatively low temperatures the same large values, $D_e \simeq 1$ cm^2/s, as at high temperatures. Taking account of true $D_e(T_e)$ dependence stabilized the model considerably.

Acknowledgements. The author is grateful to Dr. B.F. Kostenko.

References

[1] Goncharov I.N., Kostenko B.F., Philinova V.P. Phys. Lett. A 2001, **288**, p.111

[2] Kostenko B.F., Pribiš J., Goncharov I.N. Part. and Nucl., Lett. 2006, **3**, p.31

[3] Kostenko B.F., Pribiš J. Part. and Nucl., Lett. 2008, **5**, p.305

[4] Zhu Yimei et al. Phys. Rev. B 1993, **48**, p.6436

[5] Meftah A. et al. Phys. Rev. B 1993, **48**, p.920

[6] Waligorski M.P.R., Hamm R.N., Katz R. Nucl. Tracks Radiat. Meas. 1986, **1**, p.309

[7] Barashenkov V.S. Russ. Chem. of High Energies 1994, **28**, p.229

[8] Kostenko B.F., Pribish J., Filinova V.P. *Program for Calculation of the Radial Distributuion of Dose in the Neighbourhood of the Track of an Accelerated ion.* wwwinfo.jinr.ru/programs/jinrlib/dose/

[9] Ziegler J.F. SRIM 2013, www.srim.org

[10] Crommil M.F., Zettle A. Phys. Rev. B 1990, **41**, p.10978.

[11] Cohn J.L. et al. *Physical Properties of High Temperature Superconductors III.* 1992. Ed. by D.M. Ginsberg, Singapore: World Scientific

[12] Toulemonde M., Dufour C., Paumier E. Phys. Rev. B 1992, **46**, p.14362

[13] Martynenko Yu.V., Yavlinski Yu.N. Sov. Phys. Dokl. 1983, **28**, p.391 (Preprint IAE-4084/11, Moscow, 1985)

[14] Sciwietz G., Xiao G., Luderer E., Grande P.L. Nucl. Instr. and Meth. B 2000, **164-165**, p.354

[15] Allen P.P. et al. Phys. Rev. B 1994, **49**, p.9073

[16] Brorson S.D. et al. Solid State Comm. 1990, **74**, p.1305

[17] Idemoto Y., Fueki K. Jpn. J. Appl. Phys 1990, **29**, p.2729

[18] Mironova G.M. Material Science Forum 1993, **133-136**, p.847

[19] Toulemonde M., Bouffard S., Studer E. Nucl. Instr. Meth. B 1994, **91**, p.108

[20] Samarskij A.A. *Difference Schemes Theory.* 1983, Moscow: Nauka (in Russian)